

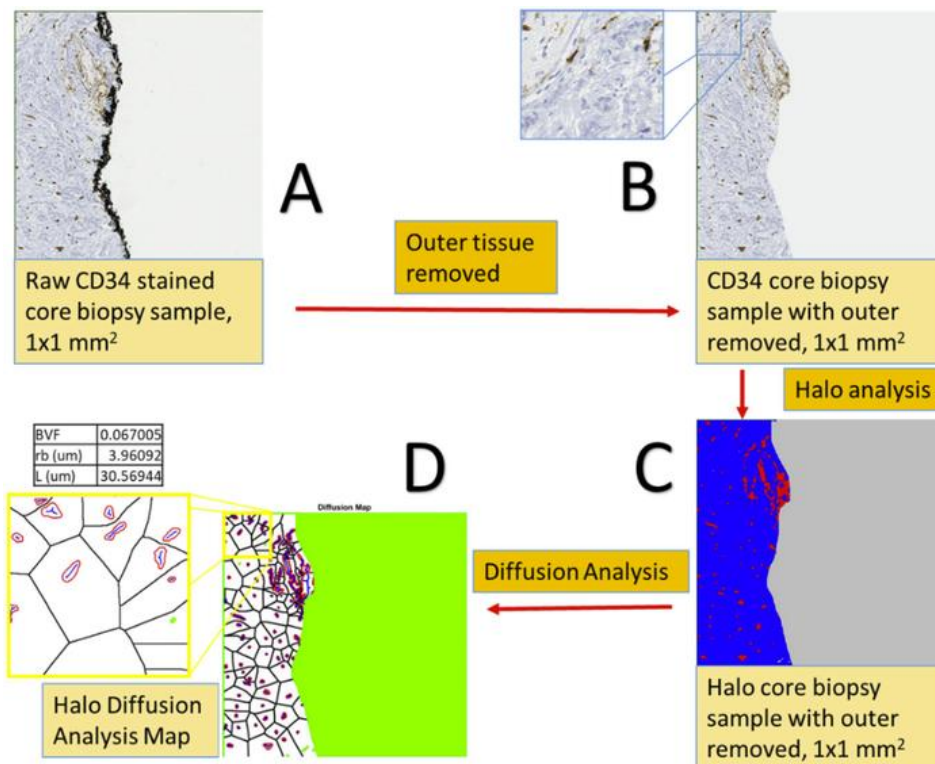
Predicting breast cancer response to neoadjuvant chemotherapy based on tumor vascular features in needle biopsies

Terisse A. Brocato, ... , C. Jeffrey Brinker, Vittorio Cristini

JCI Insight. 2019. <https://doi.org/10.1172/jci.insight.126518>.

Technical Advance In-Press Preview Oncology

Graphical abstract



Find the latest version:

<http://jci.me/126518/pdf>



Predicting breast cancer response to neoadjuvant chemotherapy based on tumor vascular features in needle biopsies

Terisse A. Brocato,^{1,†} Ursa Brown-Glaberman,^{2,†} Zhihui Wang^{3,4,†,*}, Reed G. Selwyn,^{5,6} Colin M. Wilson,⁶ Edward F. Wyckoff,⁷ Lesley C. Lomo,⁸ Jennifer L. Saline,⁶ Anupama Hooda-Nehra,^{9,11} Renata Pasqualini,^{9,10} Wadiah Arap,^{9,11,*} C. Jeffrey Brinker,^{1,7,13,14} Vittorio Cristini,^{3,4,15,*}

¹Department of Chemical and Biological Engineering and Center for Biomedical Engineering, University of New Mexico, Albuquerque, NM 87131, USA;

²University of New Mexico Comprehensive Cancer Center, Albuquerque, NM 87131, USA;

³Mathematics in Medicine Program, Houston Methodist Research Institute, Houston, TX 77030, USA;

⁴Department of Imaging Physics, University of Texas MD Anderson Cancer Center, Houston, TX 77230, USA;

⁵Center for Neuroscience and Regenerative Medicine, Uniformed Services University of the Health Sciences, Bethesda, MD 20814, USA;

⁶Department of Radiology, University of New Mexico, Albuquerque, NM 87131, USA;

⁷Center for Micro-Engineered Materials, the University of New Mexico, Albuquerque, NM 87131, USA;

⁸Department of Pathology, University of Utah, Salt Lake City, UT 84112, USA;

⁹Rutgers Cancer Institute of New Jersey, Newark, NJ 07103, USA;

¹⁰Division of Cancer Biology, Department of Radiation Oncology, Rutgers New Jersey Medical School, Newark, NJ 07103, USA;

¹¹Division of Hematology/Oncology, Department of Medicine, Rutgers New Jersey Medical School, Newark, NJ 07103, USA;

¹³Department of Molecular Genetics and Microbiology, the University of New Mexico Health Sciences Center, Albuquerque, NM 87131, USA;

¹⁴Self-Assembled Materials Department, Sandia National Laboratories, Albuquerque, NM 87185, USA;

¹⁵Department of Nanomedicine, Methodist Hospital Research Institute, Houston, TX 77030, USA.

Keywords: adenocarcinoma, mechanistic modeling, neoadjuvant chemotherapy, pre-treatment prediction, semi-automated histology analysis, translational oncology

Short title: Mathematical analysis of neoadjuvant breast cancer

Word count: 7,455

Total number of figures and tables: 7

Number of references: 32

[†]These authors contributed equally to this work.

Competing interests

The authors have declared that no competing interests exist.

Correspondence and requests for materials should be addressed to Z.W., W.A., or V.C.

*Email: zwang@houstonmethodist.org, wadih.arap@rutgers.edu, or vcristini@houstonmethodist.org

Zhihui Wang, Ph.D.

Associate Professor, Mathematics in Medicine Program
The Houston Methodist Research Institute
HMRI R8-122, 6670 Bertner Ave, Houston, TX 77030
Phone: (713) 441-7291
Email: zwang@houstonmethodist.org

Wadih Arap, M.D., Ph.D.

Director, Rutgers Cancer Institute of New Jersey
Attending Physician, Professor and Chief
Division of Hematology/Oncology
Department of Medicine
Rutgers New Jersey Medical School
Newark, NJ 07103
Phone: (973) 972-0366
Email: wadih.arap@rutgers.edu

Vittorio Cristini, Ph.D.

Professor and Director, Mathematics in Medicine Program
The Houston Methodist Research Institute
HMRI R8-123, 6670 Bertner Ave, Houston, TX 77030
Phone: (505) 934-1813
Email: vcristini@houstonmethodist.org

Abstract

In clinical breast cancer intervention, selection of the optimal treatment protocol based on predictive biomarkers remains an elusive goal. Here, we present a modeling tool to predict the likelihood of breast cancer response to neoadjuvant chemotherapy using patient specific tumor vasculature biomarkers. A semi-automated analysis was implemented and performed on 3990 histological images from 48 patients, with 10–208 images analyzed for each patient. We applied a histology-based model to resected primary breast cancer tumors ($n = 30$), and then evaluated a cohort of patients ($n = 18$) undergoing neoadjuvant chemotherapy, collecting pre- and post-treatment pathology specimens and MRI data. We found that core biopsy samples can be used with acceptable accuracy ($r = 0.76$) to determine histological parameters representative of the whole tissue region. Analysis of model histology parameters obtained from tumor vasculature measurements, specifically diffusion distance divided by radius of drug source (L/r_b) and blood volume fraction (BVF), provides a statistically significant separation of patients obtaining a pathologic complete response (pCR) from those that do not (Student's t -test; $p < 0.05$). With this model, it is feasible to evaluate primary breast tumor vasculature biomarkers in a patient specific manner, thereby allowing a precision approach to breast cancer treatment.

List of Abbreviations

AC: Doxorubicin (Adriamycin) and cyclophosphamide, chemotherapy agents

BVF: Blood volume fraction, ratio of blood vessel-to-tissue area in histopathology, or from MRI

CPS+EG: Pretreatment clinical stage and post-treatment pathologic stage (CPS score) as well as estrogen receptor status and tumor grade (EG) scores

MCE-MRI: Multiphase contrast-enhanced magnetic resonance imaging

DCE-MRI: Dynamic contrast-enhanced magnetic resonance imaging

DFS: Disease-free survival

ER, PR, HER2: Tumor receptor status for estrogen, progesterone, and human epidermal growth factor 2

f_{kill} : Fraction of dead tumor, calculated as a function of L , r_b , and BVF

L : Diffusion penetration distance, the distance drug may diffuse away from a vessel and into the surrounding tissue at clinically useful concentrations

OS: Overall survival

pCR: Pathologic complete response

r_b : Radius of drug source, blood vessels in the tumor region

ROI: Region of interest

T: Paclitaxel (Taxol), a chemotherapy agent

TILs: Tumor infiltrating lymphocytes

TN: Triple negative hormone receptor status, tumor is negative for ER, PR, and HER2 receptors.

Introduction

In the United States, breast cancer is the most common female cancer and is the second most common cause of cancer death in women (1). While major advances have been achieved in treatment of early stage breast cancer, many women still die from metastatic disease. The use of neoadjuvant chemotherapy has recently emerged as a promising method to increase treatment efficacy in patients with early stage breast cancer, with improved patient survival shown to be correlated with complete eradication of invasive tumor in the primary breast lesion and lymph nodes (pathologic complete response, pCR) upon surgery following neoadjuvant chemotherapy. This has been demonstrated in multiple clinical trials, including National Surgical Adjuvant Breast and Bowel Project (NSABP) protocol B18, in which 1,523 women with early stage breast cancer were randomly assigned to preoperative versus postoperative anthracycline-based chemotherapy (2). There was no difference in disease-free survival (DFS) or overall survival (OS) at 5 years between treatment groups. However, in the 683 women that received neoadjuvant treatment, outcomes were significantly better in women who achieved pCR compared to those without pCR (5 year OS 87.2% vs. 76.9–78.4%, $p = 0.06$; DFS 83.6% vs. 60.3–71.7%, $p = 0.0004$) after neoadjuvant therapy (3). Response to chemotherapy and pCR rates are known to vary by breast cancer subtype and chemotherapy regimen. This caveat notwithstanding, pCR has been shown to be a suitable surrogate endpoint for survival in patients with high-risk ER positive/HER2-negative (i.e., luminal B), HER2 positive (nonluminal), and triple-negative disease, though not for those with low-risk ER positive/HER2-negative (luminal A) breast cancer (4). Data also support that women who have a response to neoadjuvant chemotherapy but do not achieve a pCR have improved long-term outcomes when compared to those who do not respond,

by using response in the primary breast lesion as a surrogate for chemosensitivity. Mittendorf et al. described and validated a novel breast cancer staging system for assessing prognosis after neoadjuvant chemotherapy on the basis of pretreatment clinical stage (CS), post-treatment pathologic stage (PS), and estrogen receptor status and grade (EG), known as the CPS+EG score (5). The ability of the CPS+EG score to stratify outcome was confirmed in both internal and external cohorts, with a score of ≤ 2 corresponding with a 5-year disease-specific survival (DSS) ranging from 88% to 96%, while DSS was reduced with a score of ≥ 3 , ranging from 72–88% (5).

Neoadjuvant cytotoxic chemotherapy with an anthracycline plus taxane-based regimen, recommended as a preferred regimen by the National Comprehensive Cancer Network, results in a pCR in only a minor subset of patients (6). For example, in SWOG 0012, 185 patients with locally advanced breast cancer were treated with standard doxorubicin (Adriamycin) plus cyclophosphamide (AC) given every 21 days for 5 cycles, followed by weekly paclitaxel (T) for 12 weeks (8). Overall pCR rate was 21%. However, in patients with hormone receptor (HR)-negative tumors, the pCR rate was 29% compared to 11% in patients with HR-positive tumors. Tumor specific biomarkers for predicting response have been explored, including tumor-infiltrating lymphocytes (TILs). TILs correlate with improved outcomes in several cancer types, including colorectal, ovarian, esophageal, renal, lung, pancreatic, and breast cancer (9, 10). Specific to early-stage breast cancer (of particular interest for this work), the presence of TILs in diagnostic needle core biopsy was shown to be an independent predictor of response to neoadjuvant chemotherapy (11), as was TIL density (12). Unfortunately, our clinical ability to *a priori* predict pCR to neoadjuvant therapy in breast cancer patients remains limited at best.

Therefore, in order to maximize the utility of the neoadjuvant therapy strategy in multiple breast cancer subtypes, there is a clinical unmet need for tools to identify patients that are likely to respond to neoadjuvant cytotoxic chemotherapy, thereby allowing a precision approach to cancer treatment.

Over the years, our group has proposed that the characteristics of the tumor vasculature might be a biologic predictor of response to chemotherapy. This mechanistic hypothesis has been examined in a series of modeling studies to evaluate the prediction of treatment outcomes based on chemotherapy drug diffusion and the physical properties of several tumor types (13-29). We and other investigators have proposed that diffusion barriers may prevent drugs from reaching malignant tumor cells, a functional mechanism that might partially underlie drug resistance (30). Our mathematical model for predicting tumor response to chemotherapy (denoted by f_{kill} , i.e., the fraction of tumor killed due to therapy) has been retrospectively validated in patients with colorectal cancer (CRC) with metastasis to the liver (13). In metastatic CRC, the model predicted tumor response to chemotherapy using three drug perfusion- and diffusion-related parameters: blood volume fraction (BVF) in the tumor, the distribution of blood vessels (r_b), and the drug diffusion distance in tumor tissue (L); such parameters were tumor- and patient-specific, and thus were measured on an individual basis.

In this work, we have reasoned that the microanatomic cancer environment and functional attributes of the tumor-associated vasculature might be a biologic predictor of response to neoadjuvant chemotherapy in the setting of human breast cancer. We set out to test, validate, and expand our predictive mathematical model by rigorously applying it to three prospective cohorts

of human breast cancer patients through an integrated evaluation of histopathology and multiphase contrast-enhanced magnetic resonance imaging (MCE-MRI) data with a computer-assisted semi-automated software to enable rapid yet robust throughput that may be adapted to routine clinical imaging settings.

Results

Needle Core Biopsy Feasibility

An overview of our research protocol is depicted (**Figure 1**). We sought to determine the feasibility of using diagnostic needle core biopsies to inform a mathematical model for prediction of f_{kill} in women with infiltrating ductal adenocarcinoma of the breast receiving neoadjuvant anthracycline/taxane-based combination cytotoxic chemotherapy. As an initial step towards this goal, histopathological analysis to obtain model parameters was performed retrospectively on whole tumors from a cohort of breast cancer patients ($n = 30$, termed Cohort A) who underwent upfront either lumpectomy or mastectomy (primary surgery without prior systemic cytotoxic therapy). For Cohort A, we chose to evaluate the spectrum of breast cancer, including ER/PR positive, HER2 positive, and triple-negative breast cancer. There was no detectable differentiation between patient groups (hormone receptor-positive tumors, HER2-positive, and triple-negative breast cancer) in Cohort A with regards to model parameters by an ANOVA test (**Figure S1**).

Model parameters obtained from whole tumors in Cohort A patients were subsequently compared to a similar analysis of histopathologic samples from diagnostic needle core biopsies of a second cohort ($n = 18$, termed Cohort B) of high-risk Stage II and III HER2-negative breast cancer (i.e., triple-negative and high-risk ER positive/HER2) treated with neoadjuvant anthracycline/taxane-based chemotherapy (**Figure 2**). We found that Cohort A had a higher BVF than Cohort B, presumably due to the whole tumor section analysis in Cohort A relative to the limited core biopsy samples in Cohort B. Due to shape alone, the tissue section from a whole

tumor section results in a larger highly vascularized tissue region (perimeter of tumor) for Cohort A when compared to the cylindrical shape of a core biopsy for Cohort B. This analysis also indicated that vasculature characteristics must be measured on an individual basis in breast cancer. We then performed nonlinear regression by fitting the f_{kill} model to one of the patient histological parameters (i.e., BVF) specific to the tumor vasculature of each patient to determine the best fit for L/r_b for the entire dataset. We found that the patient samples for both cohorts fall along the same regression line (**Figure 2**); see fitting results in the inset. A correlation analysis between $f_{\text{kill}} [\text{BVF}_{\text{biopsy}}, (L/r_b)_{\text{biopsy}}]$ versus $f_{\text{kill}} [\text{BVF}_{\text{biopsy}}, (L/r_b)_{\text{fitting}}]$ for Cohort B resulted in $r = 0.7042$. Hence, we have concluded that needle core biopsy samples may indeed be used to reliably determine histopathological parameters representative of the whole tissue.

Separation between Clinical Outcomes by L/r_b

The CPS+EG score, used as a method to quantify response to neoadjuvant chemotherapy, ranges from 0–6, with a CPS+EG score ≤ 2 corresponding to a 5-year DSS from 88% to 96% (5). Our model was unable to discriminate between responders and non-responders in Cohort B by using a CPS+EG score of ≤ 2 to define response. However, analysis of histopathology measurements, specifically L/r_b , has provided a statistically significant separation of patients achieving a pCR from those that do not ($p = 0.0269$) (**Figure 3**). We note that the obtained accuracy cannot be fully ascertained due to the small sample size, but the feasibility of using the parameter L/r_b to separate patients can be observed and further examined in future larger trials. We also note that all of the patients achieving a pCR in Cohort B had triple-negative breast cancer. A single patient was identified as a clear outlier, likely due to its dense population of TILs (not shown), an

independent predictor of response to neoadjuvant chemotherapy (11, 12). Similar dense TIL infiltrates were not identified in the other 17 patients in Cohort B.

MCE-MRI Area under the Curve Association to Histology L/r_b

To evaluate model parameters via MRI, an area under the curve (AUC) map in the tumor region was used to estimate tumor blood perfusion from MCE-MRI data, as described by Pickles et al. (31). In order to obtain quantitative data from MCE-MRI, a region of interest (ROI) must first be defined; here, the hotspot of the tissue ROI (tumor or control tissue) was used to determine the maximum perfusion in that tissue region (see **Figure S7** for visualization of hotspot). The hotspot region of the tumor was normalized to tissue in the equivalent anatomical location at the mirrored location on the contralateral breast (which represents a normal tissue region); this normalized value was used for analysis shown in **Figure 4**. Correlation between AUC as determined by MCE-MRI and L/r_b as calculated by diagnostic needle core biopsy is shown in **Figure 4**. As described above, in Cohort B, L/r_b demonstrates a positive correlation with pCR (i.e., the larger the L/r_b value, the better the chance is to achieve a pCR; see **Figure 3**). Our current analysis is limited by small sample size but these pilot results that suggest a potential correlation between AUC and L/r_b are encouraging. AUC may be assessed without core biopsy samples, a potential benefit given the limited specimen size obtained at the time of diagnostic biopsy and the increasingly common acquisition of pre-treatment breast MRI in women receiving neoadjuvant chemotherapy. We further compared model predictions from histopathology data only [i.e., f_{kill} (histology)] with that from MRI data only [i.e., f_{kill} (MRI)], and observed a weak correlation between these two predictions (**Figure S5**). To further determine whether there exists a statistically significant correlation between f_{kill} (histology) and f_{kill} (MRI), a

larger data set beyond the scope of this initial report will be required in future prospective studies.

Discussion

We have demonstrated the feasibility of evaluating breast cancer vasculature in a patient-specific manner with a customized semi-automated analysis. The quantities: r_b , BVF, and L are shown to be reliably predictive of tumor f_{kill} when obtained from standard diagnostic needle core biopsy in stage II-III breast cancer patients, particularly in those with triple-negative breast cancer achieving a pCR. Application of this model for clinical use at the initial diagnostic stage may allow non-invasive prediction of outcome, whereby likelihood of pCR can be estimated early in the course of treatment, by using the flowchart depicted in **Figure 5**. The pilot framework introduced here represents the steps towards the design of a subsequent larger prospective trials with our mathematical model to potentially select neoadjuvant chemotherapy treatment based on predicted response, treating only those patients most likely to have a response with standard anthracycline/taxane-based chemotherapy, while referring those unlikely to respond to other standard of care options (e.g., radiation therapy) or even investigational clinical trials.

Tumor vasculature is a chaotic labyrinth of malformed and destabilized blood vessels that are structurally and functionally impaired (32). Jain has argued that drug delivery to tumors could be enhanced through tumor blood vessel normalization and reduced interstitial fluid pressure induced by anti-angiogenic therapy (33). Along those lines of reasoning, a high L/r_b value in patients achieving a pCR is likely indicative of a more “normalized” baseline tumor vasculature, perhaps explaining improved response to chemotherapy in this subset of patients. A higher L/r_b value suggests that chemotherapy drugs may be more effectively delivered in these solid tumors, resulting in an improved kill fraction. Normal tissue has regularly spaced (or separated) blood

vessels which increases the value L , and thus an increased L/r_b as well. Patient tumors with a high L/r_b values tended to have “pooled blood,” or regions with highly vascularized tissue, severely limiting blood and drug delivery to poorly vascularized tumor regions. Model parameters correlated with pCR following neoadjuvant chemotherapy in women with triple-negative breast cancers, but they did not correlate with a less than complete response (i.e., CPS+EG score ≤ 2) in triple-negative or high risk ER positive/HER2-negative breast cancers. We attribute this, in part, to our relatively small breast cancer patient population in the setting of a proof-of-concept study of a notoriously heterogeneous human tumor. Evaluation of our enabling mathematical platform in a larger breast cancer patient population might potentially allow the incorporation of other biologic features, including intensity of ER/PR expression, Ki67, grade, and presence of TILs, to aid in predicting response to chemotherapy, particularly in those patients destined to achieve less than a pCR.

Several technical aspects of the methodology merit further discussion. To begin, one of the limitations in our previous research in CRC (13) was that the histopathology parameters L and r_b were solved for in the f_{kill} model, while BVF was previously measured from hematoxylin and eosin-stained slides (13). Here, we have updated and refined this methodology by measuring these values (L , r_b , and BVF) directly from tissue sections, utilizing vasculature-specific staining to enable better visualization, increasing the accuracy of analysis. Measurements were previously done manually, which is both cumbersome and prone to human operator error. In contrast, a computer-assisted software program was customized here to allow for increased accuracy and speed in measurements; the semi-automated analysis allowed for rapid throughput, and a total of 3990 patient images were analyzed. Moreover, in this work we have correlated clinically

relevant treatment response assessments (pCR and CPS+EG score) with model parameters measured. Other limitations include differences in tumor vasculature staining via immunohistochemistry, although this source of bias has been greatly minimized through an automated staining protocol. Finally, while the chemotherapy regimen used was internally consistent, we have included all HER2-negative patients, resulting in a far more diverse patient population and thus increased heterogeneity in terms of response to neoadjuvant chemotherapy.

While we present exploratory data regarding the use of breast MRI to obtain model parameters, additional optimization is needed in future work. The clinical MRIs evaluated in this study were acquired with routine clinical protocols, which are focused on optimizing workflow and clinical radiology reporting instead of quantitative assessment for precision medicine. However, based on the pilot MRI data presented, AUC estimated from MCE-MRI analysis provided encouraging information regarding patient response. In our evaluation, hotspot ROI AUC analysis had the best correlation to treatment outcomes, when compared to looking at the whole tumor with 3D spherical ROI and a tumor ROI. Thus, the highest perfused region seems to be the best predictor of treatment outcomes. There is a growing demand for and a body of evidence supporting development of precision imaging models. For the purposes of model parameter determination, MCE-MRIs should ideally contain a normalization method during acquisition to allow for a controlled method for T1 and B1 mapping (34). In order to obtain BVF from breast MRI, arterial input function might be evaluated at the time of scanning, with the ultimate inspirational goal of eliminating the need for needle core biopsy analysis for model prediction.

The semi-automated histology analysis described here can potentially be used for other solid tumors, although thresholding based on vascular staining and tumor types may need to be optimized for each. The general applicability of the mechanistic f_{kill} model to predict response in several other cancer types has been examined and confirmed, including CRC with metastasis to liver, glioblastoma, pancreatic cancer, and lymphoma (13, 16, 18, 21). The observed consistency across tumor types is attributed to the fact that the f_{kill} model was derived from fundamental principles of mass transport common to many solid tumor types (13), and evaluates vasculature characteristics in the tumor prior to treatment, thereby determining the efficiency of the vascular network to deliver drugs to the tumor. Our next steps will expand upon these results through inclusion of a large-scale dataset containing more MRI measurements with additional time points, along with additional tumor parameters to predict response.

In summary, we report a mathematical modeling framework validated in patients with breast cancer from a single-institution study that will be reproduced and further investigated in a large multi-institutional setting. If successful, the hypothesis-generating results introduced here may enable the future development of minimally-invasive tools to accurately predict tumor response to neoadjuvant chemotherapy in human breast cancer patients.

Methods and Materials

Patient Cohorts. Cohort A: The first step in evaluating our model in breast cancer was to analyze model parameters in primary resected breast tumors. We used primary resected tumors initially, as this provided ample tissue for histologic evaluation. In addition, we chose to evaluate a variety of breast cancer subtypes with regards to estrogen receptor, progesterone receptor and HER2 expression, as it was unknown if model parameters would vary by biomarker status. Thus, in Cohort A, we retrospectively determined the parameters r_b , BVF, and L from primary resected breast tumors, reviewing hormone (estrogen and progesterone) receptor-positive tumors ($n = 10$), HER2-positive tumors ($n = 10$), and tumors negative for both hormone receptors and HER2 (triple-negative, $n = 10$) utilizing de-identified archival paraffin-embedded tissue.

Cohort B: After determination of model parameters in Cohort A, the model was applied to women who received neoadjuvant chemotherapy (Cohort B). Cohort B ($n = 18$), as summarized in **Table 1**, consisted of women with HER2-negative high-risk stage II-III infiltrating ductal carcinoma of the breast receiving neoadjuvant chemotherapy with a modern anthracycline / taxane-based regimen. High-risk was based on stage and the opinion of the treating provider (and Tumor Board) that neoadjuvant chemotherapy was warranted. As model parameters did not vary by biomarker status in Cohort A, in Cohort B we focused on exclusively HER-2 negative patients to increase homogeneity with regards to chemotherapy regimen. In Cohort B, paraffin-embedded baseline diagnostic needle core biopsy of primary breast tumor pre-chemotherapy was used to determine model parameters r_b , BVF, and L via semi-automated histopathology analysis as discussed below. In Cohort A, we used whole tumor for analysis, and found model

parameters consistent across the tumor section despite tumor heterogeneity (as described below, identifying tumor, stroma, and vasculature). Thus, we felt confident moving to needle core biopsy alone for analysis in Cohort B. In addition, in Cohort B pre- and post-chemotherapy MRI, performed per standard-of-care, were used to obtain model parameters via an alternative imaging-based method (detailed below). Following neoadjuvant chemotherapy, all patients underwent surgical resection, allowing assessment of pathologic response and calculation of CPS+EG score.

Patient Outcome Evaluation. Patient treatment response was determined after completing neoadjuvant chemotherapy. Resected specimens were analyzed for pCR (yes/no). In addition, patient treatment response was assessed by using the CPS+EG score (5). Calculation of CPS+EG score was performed by the study team based on presenting clinical stage (obtained from pre-treatment clinical notes), histologic grade and estrogen receptor status (determined by routine pathology review of pre-treatment diagnostic biopsy), and post-neoadjuvant chemotherapy pathologic stage (determined by routine pathology review of post-treatment resection specimen) as described in (5). Patient response was defined and analyzed by (i) pathologic complete response (pCR): no evidence of viable residual tumor in the primary resected breast specimen following the completion of neoadjuvant chemotherapy, and (ii) CPS+EG score ≤ 2 .

Magnetic Resonance Imaging. Patients had pre-treatment and post-treatment gadolinium MCE MRI scans on a 3T MRI (Siemens, Magnetom Tim Trio), which served as an imaging method to determine tumor and breast tissue perfusion. MRIs were obtained as part of routine clinical care prior to the administration of neoadjuvant chemotherapy (pre-treatment) and after all planned

neoadjuvant chemotherapy was administered prior to surgery (post-treatment). Baseline axial 3D gradient echo-based (FLASH) T1 scans were acquired without contrast using a dedicated 7 channel, receive-only breast coil with fat saturation and with the following parameters: 12-degree flip angle, 3.88/1.54 msec TR/TE, .9 mm slice thickness, 488 × 358 FE/PE matrix. Post contrast images were acquired with the same parameters as baseline images with Magnevist (0.2 ml/kg, 2 ml/sec) administered intravenously, with image acquisition at 1.5 minutes, 3.5 minutes, and 5.5 minutes post injection. Three subtraction images were created (post-pre) and used for MRI analysis. Patients with MRIs not conforming to these criteria were excluded from the MRI analysis. Analysis of MRI data was performed with OsiriX Dynamic Contrast-Enhanced (DCE) Tool Plugin (35). Area under the curve was measured by using a 3D spherical ROI over the tumor region determined by an index radiologist attending, and the hotspot (maximum signal in a 1 cm³ region given the original ROI) was measured for the tumor. For normalization, a control ROI was assessed on the contralateral breast in the same general anatomical position as the tumor, considered a baseline for the individual normal tissue vasculature in each patient. **Figure S7** depicts representative MRI images along with the analyses performed.

Histopathology. Patient tissue samples were formalin-fixed and paraffin embedded, and processed per institutional standard of care, in compliance with the American Society of Clinical Oncology/College of American Pathology (ASCO-CAP) guidelines. The Human Tissue Repository and Tissue Analysis Shared Resource at the University of New Mexico Comprehensive Cancer Center (UNMCCC) served as an honest broker for access to all tumor specimens. CD34 antibody staining via immunohistochemistry was used to highlight tumor

vasculature, and H&E staining was performed to evaluate tissue morphology (e.g. tumor versus non-tumor).

Histopathology Semi-automated Analysis. Representative single sections of primary resected tumor for patient Cohort A, and representative single sections from needle core biopsy samples from patient Cohort B were analyzed by using HALO image analysis software (Indica Labs) to separate tissue regions in the CD34 stained tissue sections into CD34-positive tissue regions (vasculature), CD34-negative tissue regions (non-vasculature tissue), and background regions (non-tissue). HALO uses machine-learning to classify tissue regions based on a training set. Tissue regions were separated into $1 \times 1 \text{ mm}^2$ square regions for analysis using code developed in Matlab (MathWorks). This code takes the HALO-separated regions and measures vasculature radius, r_b (μm), measured along the short axis of the blood vessel due to the consideration that the blood vessel could be in the plane of the tissue section, thus ensuring we do not overestimate this parameter (**Figure 6**). Multiple measurements were taken for each blood vessel and averaged to obtain a single r_b value for each grid analyzed. To ensure the accuracy of the semi-automated methods developed, each measurement was checked multiple times over multiple iterations of the software analysis. The blood volume fraction, BVF, was taken to be the vasculature area (in red) divided by the whole tissue region (**Figure 6C, blue + red**). Only tissue regions were considered for BVF measurement. Vessels were assumed to supply drug and nutrients to all surrounding tissue that was nearest to that vessel, these perimeters define the maximum diffusion length L , and are shown in black (**Figure 6D**). The distances between this boundary (black) and the nearest blood vessel (in red) were measured and averaged for each grid analyzed to get the diffusion penetration distance L (μm). We note here that larger blood vessels (which are

presumably expected to deliver greater amounts of drug) increase the r_b value, thus decreasing L/r_b . This is balanced by L , which may have a longer penetration distance due to the increased vascular supply. In other words, it is the ratio of these two quantities that must be considered together instead of individually when evaluating treatment efficacy.

Mathematical Model.

$$f_{\text{kill}} = 2 \cdot \text{BVF} \cdot \frac{\sqrt{\text{BVF}} \cdot K_1(r_b/L) - K_1(r_b/(L \cdot \sqrt{\text{BVF}}))}{\sqrt{\text{BVF}} \cdot r_b / L \cdot K_0(r_b/L) \cdot (1 - \text{BVF})} \quad [1]$$

The f_{kill} equation with parameters r_b , BVF, and L , which are directly measured from histology semi-automated analysis. f_{kill} is the fraction of tumor cells killed, r_b is the average radius of blood vessels in the tissue section analyzed, BVF is the fraction of blood volume in the tumor, and L is the farthest distance nutrients/drug need to travel from a blood vessel to reach all tissue (13).

Statistics. Matlab and GraphPad Prism 7 were used to determine best fits of patient averages for BVF, r_b and L placed into Eq. 1 and by using non-linear regression solving for L/r_b . Fits were obtained with initial values for fit, $L/r_b = 20$ and $L/r_b > 0.005$ for a constraint. For data in **Figure 3**, a two-tailed Student's t-test was used to compare histopathology measurements (L/r_b) from the two groups (pCR and no pCR). $p < 0.05$ was considered statistically significant.

Study approval. For all components of this research, approvals were obtained from the IRB of the University of New Mexico Health Sciences Center, study ID numbers 14-070 and 15-017.

Studies were conducted according to the principles set out in the Declaration of Helsinki. Written informed consent was obtained from all prospective study patients.

Author contributions

TAB performed histopathology analysis, MRI analysis, code development, and interpreted and analyzed the data. UBG, LCL, JLS, and VC initiated the project and designed patient treatment protocol. UBG, LCL, and JLS performed cancer care and patient trial enrollment. UBG and LL provided human tissues and supervised human histopathological data interpretation. ZW supervised data analysis, code development, and modeling. RGS and CMW participated in MRI analysis and interpretation. EFW provided assistance in histological data analysis and code development. AH, RP, WA, and CJB participated in data analysis. ZW, RP, WA, and VC coordinated and supervised the overall research effort. TAB, UBG, ZW, RP, WA, and VC wrote the manuscript.

Acknowledgements

We thank trial participants and study clinicians. We also give thanks to the Human Tissue Repository and Fred Schultz for his contribution in using the HALO system at the University of New Mexico. This research was supported by the National Cancer Institutes and the Cancer Center Support Grant through Grant P30CA118100. This research has also been supported in part by the New Mexico Cancer Nanoscience and Microsystems Training Center (CNTC) Graduate Student Fellowship (TAB); the National Science Foundation Grant DMS-1716737 (ZW, VC), the National Institutes of Health (NIH) Grants 1U01CA196403 (ZW, VC), 1U01CA213759 (ZW, VC), 1R01CA226537 (ZW, RP, WA, CJB, VC), 1R01CA222007 (ZW, VC), U54CA210181 (ZW, VC), and the University of Texas System STARS Award (VC). Sandia National Laboratories is a multi-mission laboratory managed and operated by National

Technology and Engineering Solutions of Sandia, LLC, a wholly owned subsidiary of Honeywell International, Inc., for the U.S. Department of Energy's National Nuclear Security Administration under contract DE-NA0003525. This paper describes objective technical results and analysis. Any subjective views or opinions that might be expressed in the paper do not necessarily represent the views of the U.S. Department of Energy or the United States Government. The funders had no role in study design, data collection and analysis, decision to publish, or preparation of the manuscript.

References

1. Miller, K.D., Siegel, R.L., Lin, C.C., Mariotto, A.B., Kramer, J.L., Rowland, J.H., Stein, K.D., Alteri, R., and Jemal, A. 2016. Cancer treatment and survivorship statistics, 2016. *CA Cancer J Clin* 66:271-289.
2. Wolmark, N., Wang, J., Mamounas, E., Bryant, J., and Fisher, B. 2001. Preoperative chemotherapy in patients with operable breast cancer: nine-year results from National Surgical Adjuvant Breast and Bowel Project B-18. *J Natl Cancer Inst Monogr* 2001:96-102.
3. Fisher, B., Bryant, J., Wolmark, N., Mamounas, E., Brown, A., Fisher, E.R., Wickerham, D.L., Begovic, M., DeCillis, A., Robidoux, A., et al. 1998. Effect of preoperative chemotherapy on the outcome of women with operable breast cancer. *J Clin Oncol* 16:2672-2685.
4. von Minckwitz, G., Untch, M., Blohmer, J.U., Costa, S.D., Eidtmann, H., Fasching, P.A., Gerber, B., Eiermann, W., Hilfrich, J., Huober, J., et al. 2012. Definition and impact of pathologic complete response on prognosis after neoadjuvant chemotherapy in various intrinsic breast cancer subtypes. *J Clin Oncol* 30:1796-1804.
5. Mittendorf, E.A., Jeruss, J.S., Tucker, S.L., Kolli, A., Newman, L.A., Gonzalez-Angulo, A.M., Buchholz, T.A., Sahin, A.A., Cormier, J.N., Buzdar, A.U., et al. 2011. Validation of a novel staging system for disease-specific survival in patients with breast cancer treated with neoadjuvant chemotherapy. *J Clin Oncol* 29:1956-1962.
6. Mieog, J.S., van der Hage, J.A., and van de Velde, C.J. 2007. Preoperative chemotherapy for women with operable breast cancer. *Cochrane Database Syst Rev*:CD005002.
7. Imming, P., Sinning, C., and Meyer, A. 2006. Drugs, their targets and the nature and number of drug targets. *Nat Rev Drug Discov* 5:821-834.
8. Ellis, G.K., Barlow, W.E., Gralow, J.R., Hortobagyi, G.N., Russell, C.A., Royce, M.E., Perez, E.A., Lew, D., and Livingston, R.B. 2011. Phase III comparison of standard doxorubicin and cyclophosphamide versus weekly doxorubicin and daily oral cyclophosphamide plus granulocyte colony-stimulating factor as neoadjuvant therapy for inflammatory and locally advanced breast cancer: SWOG 0012. *J Clin Oncol* 29:1014-1021.
9. Mahmoud, S.M., Paish, E.C., Powe, D.G., Macmillan, R.D., Grainge, M.J., Lee, A.H., Ellis, I.O., and Green, A.R. 2011. Tumor-infiltrating CD8+ lymphocytes predict clinical outcome in breast cancer. *J Clin Oncol* 29:1949-1955.
10. Denkert, C., von Minckwitz, G., Brase, J.C., Sinn, B.V., Gade, S., Kronenwett, R., Pfitzner, B.M., Salat, C., Loi, S., Schmitt, W.D., et al. 2015. Tumor-infiltrating lymphocytes and response to neoadjuvant chemotherapy with or without carboplatin in human epidermal growth factor receptor 2-positive and triple-negative primary breast cancers. *J Clin Oncol* 33:983-991.
11. Denkert, C., Loibl, S., Noske, A., Roller, M., Muller, B.M., Komor, M., Budczies, J., Darb-Esfahani, S., Kronenwett, R., Hanusch, C., et al. 2010. Tumor-associated lymphocytes as an independent predictor of response to neoadjuvant chemotherapy in breast cancer. *J Clin Oncol* 28:105-113.
12. Ali, H.R., Dariush, A., Provenzano, E., Bardwell, H., Abraham, J.E., Iddawela, M., Vallier, A.L., Hiller, L., Dunn, J.A., Bowden, S.J., et al. 2016. Computational pathology

- of pre-treatment biopsies identifies lymphocyte density as a predictor of response to neoadjuvant chemotherapy in breast cancer. *Breast Cancer Res* 18:21.
13. Pascal, J., Bearer, E.L., Wang, Z., Koay, E.J., Curley, S.A., and Cristini, V. 2013. Mechanistic patient-specific predictive correlation of tumor drug response with microenvironment and perfusion measurements. *Proc Natl Acad Sci U S A* 110:14266-14271.
 14. Das, H., Wang, Z., Niazi, M.K., Aggarwal, R., Lu, J., Kanji, S., Das, M., Joseph, M., Gurcan, M., and Cristini, V. 2013. Impact of diffusion barriers to small cytotoxic molecules on the efficacy of immunotherapy in breast cancer. *PLoS One* 8:e61398.
 15. Pascal, J., Ashley, C.E., Wang, Z., Brocato, T.A., Butner, J.D., Carnes, E.C., Koay, E.J., Brinker, C.J., and Cristini, V. 2013. Mechanistic modeling identifies drug-uptake history as predictor of tumor drug resistance and nano-carrier-mediated response. *ACS Nano* 7:11174-11182.
 16. Koay, E.J., Truty, M.J., Cristini, V., Thomas, R.M., Chen, R., Chatterjee, D., Kang, Y., Bhosale, P.R., Tamm, E.P., Crane, C.H., et al. 2014. Transport properties of pancreatic cancer describe gemcitabine delivery and response. *J Clin Invest* 124:1525-1536.
 17. Brocato, T., Dogra, P., Koay, E.J., Day, A., Chuang, Y.L., Wang, Z., and Cristini, V. 2014. Understanding Drug Resistance in Breast Cancer with Mathematical Oncology. *Curr Breast Cancer Rep* 6:110-120.
 18. Frieboes, H.B., Smith, B.R., Wang, Z., Kotsuma, M., Ito, K., Day, A., Cahill, B., Flinders, C., Mumenthaler, S.M., Mallick, P., et al. 2015. Predictive Modeling of Drug Response in Non-Hodgkin's Lymphoma. *PLoS One* 10:e0129433.
 19. Wang, Z., Butner, J.D., Kerketta, R., Cristini, V., and Deisboeck, T.S. 2015. Simulating cancer growth with multiscale agent-based modeling. *Semin Cancer Biol* 30:70-78.
 20. Wang, Z., Butner, J.D., Cristini, V., and Deisboeck, T.S. 2015. Integrated PK-PD and agent-based modeling in oncology. *J Pharmacokinet Pharmacodyn* 42:179-189.
 21. Wang, Z., Kerketta, R., Chuang, Y.L., Dogra, P., Butner, J.D., Brocato, T.A., Day, A., Xu, R., Shen, H., Simbawa, E., et al. 2016. Theory and Experimental Validation of a Spatio-temporal Model of Chemotherapy Transport to Enhance Tumor Cell Kill. *PLoS Comput Biol* 12:e1004969.
 22. Cristini, V., Koay, E., and Wang, Z. 2017. *An Introduction to Physical Oncology: How Mechanistic Mathematical Modeling Can Improve Cancer Therapy Outcomes*: CRC Press.
 23. Frieboes, H.B., Chaplain, M.A., Thompson, A.M., Bearer, E.L., Lowengrub, J.S., and Cristini, V. 2011. Physical oncology: a bench-to-bedside quantitative and predictive approach. *Cancer Res* 71:298-302.
 24. Edgerton, M.E., Chuang, Y.L., Macklin, P., Yang, W., Bearer, E.L., and Cristini, V. 2011. A novel, patient-specific mathematical pathology approach for assessment of surgical volume: application to ductal carcinoma in situ of the breast. *Anal Cell Pathol (Amst)* 34:247-263.
 25. Deisboeck, T.S., Wang, Z., Macklin, P., and Cristini, V. 2011. Multiscale cancer modeling. *Annu Rev Biomed Eng* 13:127-155.
 26. Wang, Z., Bordas, V., and Deisboeck, T.S. 2011. Identification of Critical Molecular Components in a Multiscale Cancer Model Based on the Integration of Monte Carlo, Resampling, and ANOVA. *Front Physiol* 2:35.

27. Wang, Z., Deisboeck, T.S., and Cristini, V. 2014. Development of a sampling-based global sensitivity analysis workflow for multiscale computational cancer models. *IET Syst Biol* 8:191-197.
28. Brocato, T.A., Coker, E.N., Durfee, P.N., Lin, Y.S., Townson, J., Wyckoff, E.F., Cristini, V., Brinker, C.J., and Wang, Z. 2018. Understanding the Connection between Nanoparticle Uptake and Cancer Treatment Efficacy using Mathematical Modeling. *Sci Rep* 8:7538.
29. Dogra, P., Adolphi, N.L., Wang, Z., Lin, Y.S., Butler, K.S., Durfee, P.N., Croissant, J.G., Nouredine, A., Coker, E.N., Bearer, E.L., et al. 2018. Establishing the effects of mesoporous silica nanoparticle properties on in vivo disposition using imaging-based pharmacokinetics. *Nat Commun* 9:4551.
30. Adisheshaiah, P.P., Crist, R.M., Hook, S.S., and McNeil, S.E. 2016. Nanomedicine strategies to overcome the pathophysiological barriers of pancreatic cancer. *Nat Rev Clin Oncol* 13:750-765.
31. Pickles, M.D., Manton, D.J., Lowry, M., and Turnbull, L.W. 2009. Prognostic value of pre-treatment DCE-MRI parameters in predicting disease free and overall survival for breast cancer patients undergoing neoadjuvant chemotherapy. *Eur J Radiol* 71:498-505.
32. Nagy, J.A., Chang, S.H., Dvorak, A.M., and Dvorak, H.F. 2009. Why are tumour blood vessels abnormal and why is it important to know? *Br J Cancer* 100:865-869.
33. Jain, R.K. 2005. Normalization of Tumor Vasculature: An Emerging Concept in Antiangiogenic Therapy. *Science* 307:58-62.
34. Pineda, F.D., Medved, M., Fan, X., and Karczmar, G.S. 2016. B1 and T1 mapping of the breast with a reference tissue method. *Magn Reson Med* 75:1565-1573.
35. Sung, K.D., B; Rubin, D; Hargreaves, B. 2011. Quantitative Dynamic Contrast-enhanced MRI Analysis Tool. *Radiological Society of North America 2011 Scientific Assembly and Annual Meeting*.

Figures and Figure Legends

Figure 1.

1. Apply math modeling to Cohort A to identify primary resected whole tumor parameters
<ul style="list-style-type: none">• Cohort A: 30 patients with primary resected breast cancer (10 ER/PR+, 10 HER2+, 10 TN)• Measure tumor parameters: blood volume fraction BVF, blood vessel radius r_b, and diffusion distance L, and calculate f_{kill} using Eq. 1• Evaluate model parameters by ER, PR, and HER2 status
2. Apply math modeling to Cohort B core biopsy samples as a surrogate for whole tumor analysis
<ul style="list-style-type: none">• Cohort B: 18 patients treated with anthracycline/taxane based neoadjuvant chemotherapy• Measure tumor parameters from core biopsy samples: blood volume fraction BVF, blood vessel radius r_b, and diffusion distance L, and calculate f_{kill} using Eq. 1• Obtain pre-treatment perfusion measurements by diffusion contrast MRI as a proxy of tumor parameters
3. Apply model
<ul style="list-style-type: none">• Evaluate the post-neoadjuvant chemotherapy clinical response in Cohort B patients at the time of surgery, including CPS+EG clinical scores and pCR• Correlate f_{kill} with pCR and CPS+EG score• Correlate MRI results with response and histology results

Figure 1. Research protocol.

Figure 2.

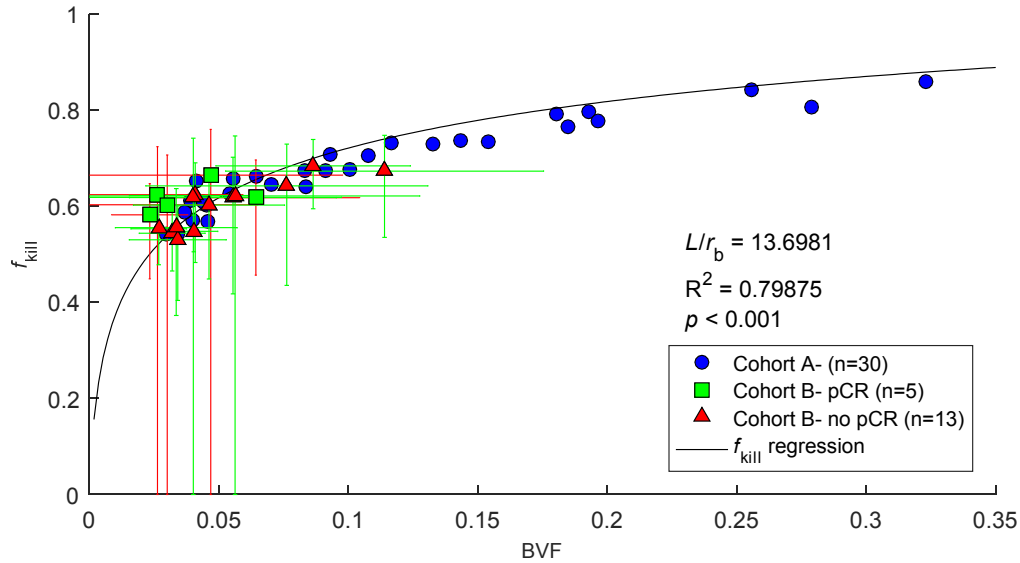


Figure 2. Model Analysis. f_{kill} values are shown as determined as 1) calculated from measured values (points; Cohort A: measured from resected whole-tumor histology, Cohort B: measured from needle biopsy) and 2) model best-fit (Eq. 1) line to the full data set (black line). Cohort A: 30 retrospective patients underwent primary surgery without prior systemic therapy analyzed by using histology semi-automated analysis and the mathematical model. Cohort B: 18 patients receiving neoadjuvant chemotherapy are shown to distinguish patients with pathologic complete response (pCR) vs. those without a pCR. Each point is f_{kill} calculated for an individual patient by using averages of BVF, r_b , and L measured directly from tumor tissue stained with CD34 by immunohistochemistry. The black line shows f_{kill} calculated from Eq. 1 with optimized parameter $L/r_b = 13.6981$ (determined from fitting, $R^2 = 0.79875$). The f_{kill} regression line includes fitting of both Cohort A and Cohort B patients ($n = 48$). Error bars are calculated based on error in BVF measurements and the respective variation that it causes when incorporated into the f_{kill} equation

(Eq. 1). Correlation analysis of measured f_{kill} and computed f_{kill} for all 48 patients is shown in **Figure S2**.

Figure 3.

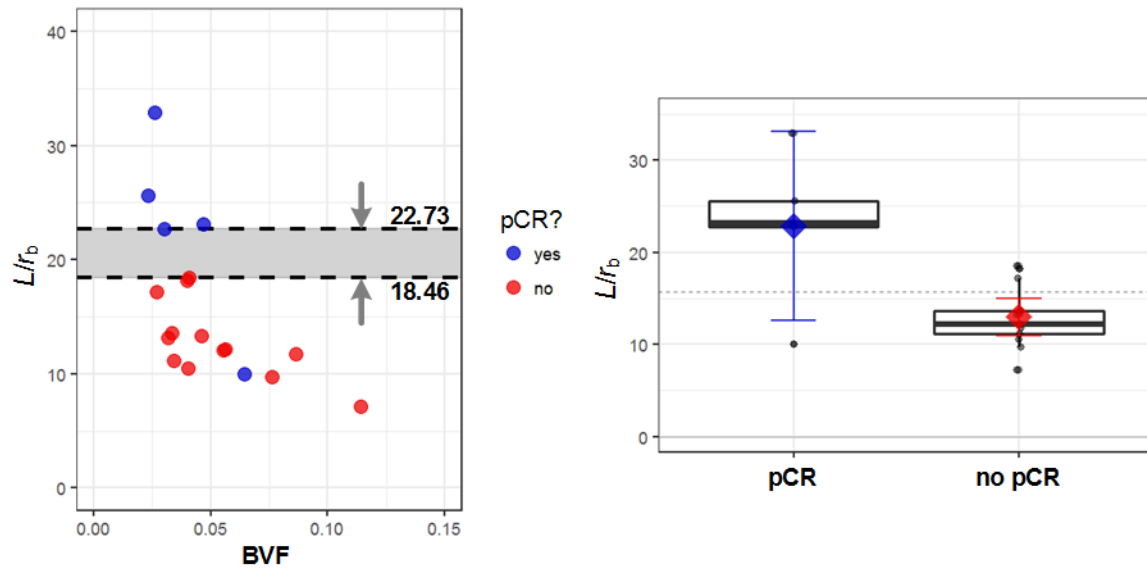


Figure 3. Histopathological parameters separate patient groups (pCR and no pCR). (left)

Patient groups can be separated by a L/r_b value within the range of 18.46 (the highest value in the “no pCR” group) and 22.73 (the 2nd lowest value in the pCR group); see the gray zone. The patient from the pCR group that has the lowest L/r_b value may be an outlier; see main text for details. (right) A Student’s t -test determined a statistically significant difference between these two groups with respect to L/r_b ($p < 0.05$).

Figure 4.

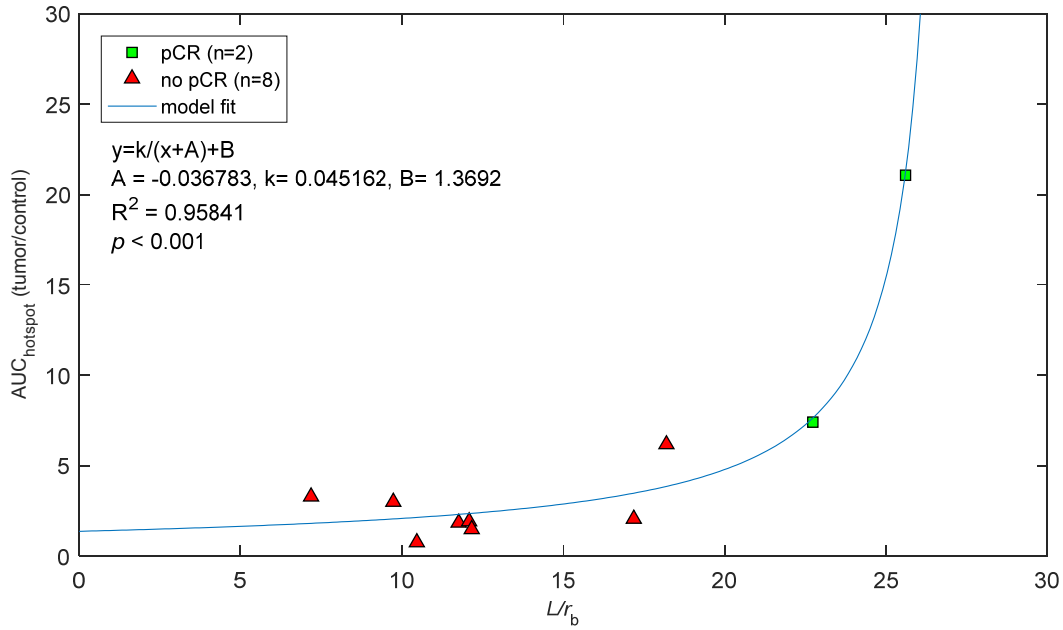


Figure 4. Response to neoadjuvant chemotherapy and MCE-MRI in Cohort B. CD34 stained core biopsy samples measured for L/r_b (radius of blood vessel: r_b , tissue diffusion penetration distance: L) and its relation to MCE-MRI area under the curve (AUC) analysis, time points 0–5.5 minutes, taken for the hotspot region of the tumor normalized to the measured healthy tissue at the mirrored anatomical location on the contralateral breast.

Figure 5.

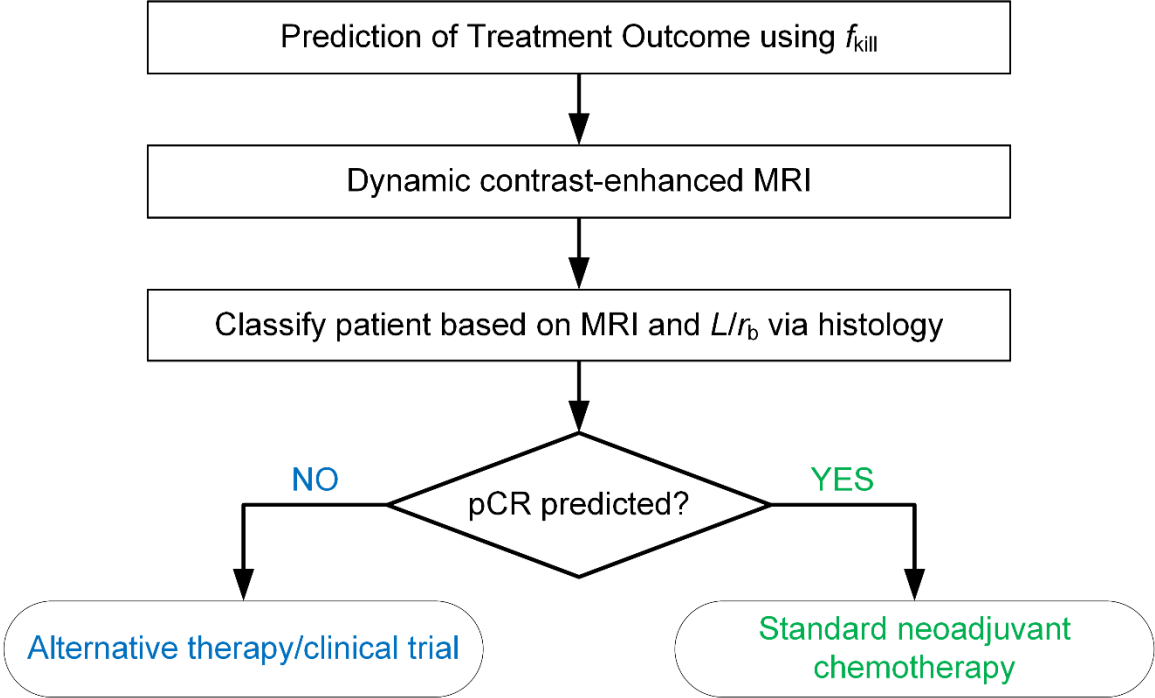


Figure 5. Prediction of treatment outcome using both MRI and tumor histology from diagnostic biopsies.

Figure 6.

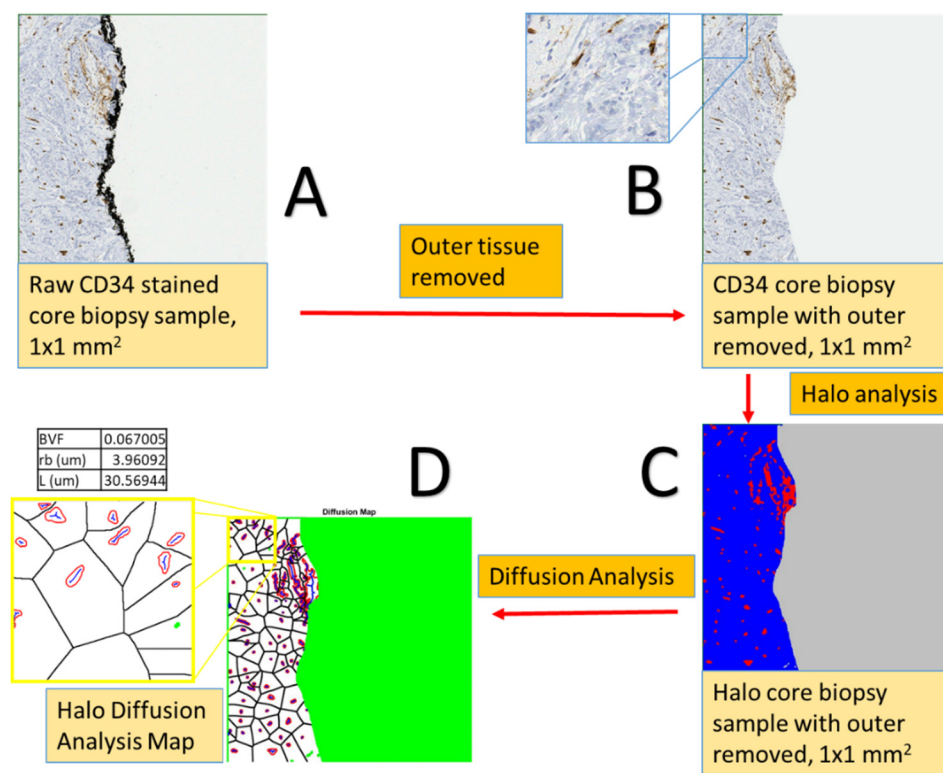


Figure 6. Diffusion analysis workflow. **A)** Shows the original CD34-stained histology grid before any processing. **B)** Displays the same tissue region as in A, but with the outer inking portion removed due to the increased likelihood of false positives on the perimeter of core biopsy samples (the pathology department inks tissue cores for quality purposes). **C)** Shows a computerized version of B with differentiation between tissue CD34⁻ (blue), vasculature CD34⁺ (red), and non-tissue regions (grey). **D)** Shows the diffusion analysis of image C, which was performed by code developed in Matlab. Parameters measured are: blood vessel radius (r_b), blood volume fraction (BVF), and diffusion distance (L). Blood vessels are outlined in red, and the total area of blood vessels in a tissue region is the blood volume fraction, BVF. The blue shows the central long axis of each vessel (multiple vessel radius measurements were taken

perpendicular to this axis). An average of all vessel radii in each image analyzed is taken to be r_b (μm). The black lines discretize the image into regions defined by having the closet proximity to the enclosed vessel; then the distance from each black boundary to the blood vessel boundary (red) is measured, and all distances averaged is the diffusion penetration distance, L , measured in μm . White is the tumor tissue region, all of which is considered for analysis. Green is the background/non-tissue region not considered for analysis.